ACS APPLIED MATERIALS & INTERFACES

RESEARCH ARTICLE

www.acsami.org

Gelation of Chitin and Chitosan Dispersed Suspensions under Electric Field: Effect of Degree of Deacetylation

Young Gun Ko,[†] Seung Su Shin,[†,‡] Ung Su Choi,[*,†] Yong Sung Park,[‡] and Je Wan Woo[‡]

[†]Energy Mechanics Center, Korea Institute of Science and Technology, 39-1 Hawolgok-dong, Wolsong-gil 5, Seongbuk-gu, Seoul 136-791, Korea

[‡]Department of Industrial Chemistry, Sangmyung University, 7 Hongji-dong, Jongno-gu, Seoul 110-743, Korea

ABSTRACT: Herein, the effect of the degree of deacetylation (DD) on the gelation of the chitosan dispersed suspension as an electrorheological (ER) fluid under an electric field is presented. The fluids were prepared by dispersing the chitin and the chitosan particles having various DDs into silicone oil, and they were evaluated under various electric fields. The alignment of chitosan particles in the fluid was also observed using an optical microscope under the electric field. The formed fibrous structure between electrodes are though to continue to the viscosity increase, because an attempt to move one electrode relative to the order would be hindered by the drag of the dangling fibrils. A noteworthy result is that the region of the frequency for gel state of the ER fluids increased in the order of chitosan DD 99.3, 93.4, 73.2, 83.8, and 87.3% under electric fields while the modulus of the fluids increased in the reverse order. This order was well-matched with the result of dielectric constants and yield stresses of ER fluids. The study of influence of DD on the gelation of the chitosan dispersed suspension under an electric field shows the relevance of the chemical composition of the heteropolysaccharide (chitin−chitosan copolymer) to the rheological and electric properties of ER suspensions.

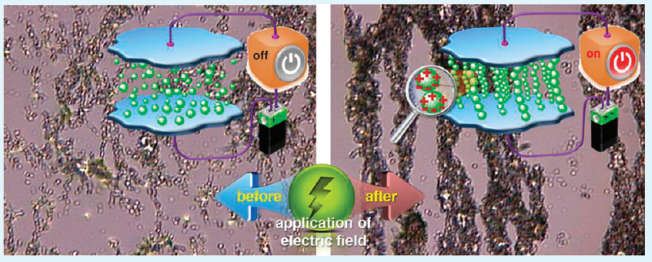

KEYWORDS: chitin, chitosan, electric field, electrorheology, gelation

INTRODUCTION

Potential applications for chitosan, such as bioinspired materials,[1] drug delivery system,[2] biosensors,[3] scaffolds for tissue engineering,[4] and so on, based on their remarkable mechanical, cytocompatible, and biocompatible properties,[5] have been intensively researched for a long time. By extension of the study on the properties of chitosan to enlarge its application, our research group have found that the viscosity of chitosan particles dispersed suspension increase with an applied electric field, and the dispersed particles are polarized and form fibrous structures under an application of an electric field.[6]

Some intelligent (smart) materials can respond to an external environmental stimulus in a timely manner, producing a useful effect.[7] The electrorheological (ER) fluids are such smart materials whose rheological properties are controllable through the application of an electric field, showing useful and special function with the effect of reversibility.[8] Because of their fast response time and controllable shear viscosity, ER fluid has been one of the most promising candidates as a new material for various industrial utilizations such as human muscle stimulators,[9] dampers,[10] seismic controlling frame structure,[11] and so on. Many efforts have been spent on developing high-performance ER materials, and many shortcomings are pertinent to these systems, for example, a narrow working temperature, solidification at low temperature, a high current density due to the high conductivity of water and device erosion caused by water.[12] Water-free ER fluids have been developed under the assumption that they do not have the shortcomings of hydrous ER fluids.[13] However, anhydrous ER fluids have different problems, particle sedimentation and nondegradable property, which could make ER fluids malfunction, environmental problems, and severely limit practical applications.[14] Enzymes (chitosanases) work in concert to achieve complete biodegradation of the chitosan.[15] Chitosan degradative enzymes are abundantly secreted into soil and water by microorganisms as part of their feeding cycle and are also present in the digestive tracts of animals. The chitosan has properties of good dispersion in an oil phase and stabilizer for an emulsion system.[16] Because of these merits such as biodegradation property, a source of abundant supply, and good dispersion-stability, we and other research groups have synthesized modified chitosans for solving the above problems.[17−21]

Chitin is the second most abundant natural biopolymer, after cellulose. Chitosan is a natural biomacromolecule produced by *N*-deacetylation of chitin, which is a natural polysaccharide.[22] Degree of deacetylation (DD) is a structural parameter which influences physicochemical properties of the chitosan, and influences the biodegradability,[23] the crystalline state,[24] the cytocompatibility,[25] the thermal decomposition,[26] the gene transfection,[27] the growth inhibitory of bacteria,[28] the dispersion for the blend with other materials,[29] and so on. Chitosan has several unique

Received: January 24, 2011
Accepted: March 14, 2011
Published: March 22, 2011

properties due to $-NH_2$ and $-OH$ group on the chitosan backbone.[30] Chitosan is polar due to these groups. The polar groups may affect the ER behavior by playing the role of the electronic donor under the imposed electric field. It has been reported in fact that the morphology of the chitosan fiber depends on DD in the electrospinning process of the chitosan.[31]

Herein, we report on the effect of the degree of deacetylation on the gelation of the chitosan dispersed suspension under an electric filed. The chitosans with the various DD levels were prepared with the alkaline treatment. Several techniques were used for the determination of DD; such as titration, CHN elemental analysis, and FT-IR spectroscopy. The electrorheological and electrical properties of the chitin and chitosan particles suspended silicone oils were investigated under DC electric fields. This paper focused on effects of DD on enhancement of electrorheological properties.

EXPERIMENTAL SECTION

Materials. Chitin from Korea red crabs and chitosan with various degree of deacetylation (DD) were purchased from YB-Bio Inc. (Korea). YB-Bio Inc. gave us information of the experimental method of deacetylation and the P.V.S.-K. titration method. The deacetylation was performed on 1 g of chitin suspended into 100 mL of 40 wt % NaOH aqueous solution and kept at 110 °C during 3 h under N_2 atmosphere. This procedure was repeated several times to get various DD levels. Afterward, the sample was abundantly washed with distilled deionized water (DI water, obtained from a Milli-Q water system as 18.2 MΩ cm^{-1}) until neutral and then dried in a vacuum oven at 50 °C for 60 h. The degree of deacetylation was determined using the P.V.S.-K. titration method.[32] The obtained values were 73.2, 83.8, 87.3, 93.4, and 99.3%. These deacetlyated chitosans were named as chitosan DD 73.2%, chitosan DD 83.8%, chitosan DD 87.3%, chitosan DD 93.4%, and chitosan DD 99.3%. The CHN analysis of deacetylated chitosans were carried out using Element Analyzer (CS 600, Leco) and DD was calculated from the following equation[33]

$$\mathrm{DD} = \left(1 - \frac{\mathrm{C/N} - 5.145}{6.861 - 5.145}\right) \times 100$$

where, C/N is carbon to nitrogen ratio. The obtained values with the CHN analysis method for chitosan DD 73.2%, chitosan DD 83.8%, chitosan DD 87.3%, chitosan DD 93.4%, and chitosan DD 99.3% were 68.7, 77.3, 86.2, 91.3, and 98.9%, respectively.

Particle Characterization. The chitin and chitosans were ground to 5−50 μm particles using a ball mill. Attenuated total reflectance Fourier transform infrared (ATR FT-IR) was used to analyze samples with a Thermo Mattson Infinity Gold 60-AR spectrometer (Thermo Electron Corp.) with a KRS-5 crystal. A mercury−cadmium-telluride (MCT) detector was used for detection. The angle of the beam was 45°. Mean particle diameter (Heywood diameter − defined as the diameter of a circle having the same area of the segmented defect) of samples was determined by a digital optical microscope (Reichert Metaplan 2, Leica) equipped with a software (Nex Measure Pro 5, Bestecvision, Korea) automatically. A field-emission scanning electron microscope (FE-SEM, HITACHIS S-4200) was used to observe the morphology of the chitosan particle.

Suspension Preparation and Electrorheological Measurements. The ER fluids were prepared by dispersing the chitin and the chitosan particles into silicone oil, whose viscosity was 30 mm^2/s at 25 °C. The silicone oil was dried using molecular sieves before use, and the particle concentration was fixed at 30 vol%. The rheological properties of the suspension were investigated in a static DC field using a Physica Couette-type rheometer (Physica MCR301) with a high-voltage generator. The measuring unit was of a concentric cylindrical type, with a 1 mm gap between the bob and the cup. The shear stress for the suspensions was measured under a shear rate of 1×10^{-5} to ∼1000 s^{-1} and electric fields of 0−3 kV/mm at 25 °C. The storage and loss moduli for the suspensions were measured under the frequency of 1×10^{-2} to 1×10^{2} Hz and electric fields of 0−3 kV/mm at 25 °C. The shear stress for the suspensions was also measured in the range of 25−100 °C at the shear rate of 100 s^{-1}.

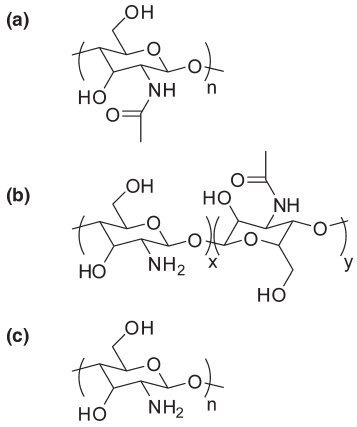

Figure 1. Chemical structures of (a) chitin, (b) chitin−chitosan hybrid polysaccharide, and (c) chitosan.

The DC current densities, J, of the chitin and chitosan suspensions were determined at room temperature by measuring the current passing through the fluid upon application of the electric field, E_0, and dividing the current by the area of the electrodes in contact with the fluid. The current was determined from the voltage drop across a 1 MΩ resistor in series with the metal cell containing the silicone oil, using a voltmeter with a sensitivity of 0.01 mV (Keithley, Model 248 High Voltage Supply). The DC conductivity was taken to be $\sigma = J/E_0$. The dielectric constants, ε, of the suspensions were measured at 1 kHz and 1000 mV using a Hewlett-Packard LCR meter (model 4263 B). Ten samples were measured in order to ensure the reproducibility of the results.

The experimental cell was assembled by mounting two parallel electrodes with a 1 mm gap on a glass slide, in which a drop of well-mixed ER fluid was dispersed. The behavior of the ER fluids was observed under 3 kV/mm using a digital optical microscope.

RESULTS AND DISCUSSION

Characterization of Chitin and Chitosan. Chitin is a high-molecular-weight heteropolysaccharide composed mainly of β-(1,4)-2-deoxy-2-acetamido-D-glucopyranose units (Figure 1a). It is not found in higher plants, but is a major constituent of crustacean exoskeletons and fungal cell walls. Purified chitin from crustacean exoskeletons, the most readily accessible form of chitin, is used for the chemical conversion of chitin to chitosan. Chitosan occurs naturally in fungi and in specialized tissues of some animals, but is difficult to isolate because it occurs covalently attached to mucopolysaccharides and proteins, or only occurs in small quantities. Though chitosan does occur naturally, it is obtained commercially by the chemical *N*-deacetylation of chitin (Figure 1c). By convention, chitin and chitosan are distinguished by their solubility in dilute organic acids. Chitosan will dissolve as a polycation in dilute acids, whereas chitin, with predominantly *N*-acetylated amine groups, will not. Chitin is the parent compound of chitosan, so the proportion of glucosamine monomer residues in chitosan is typically described

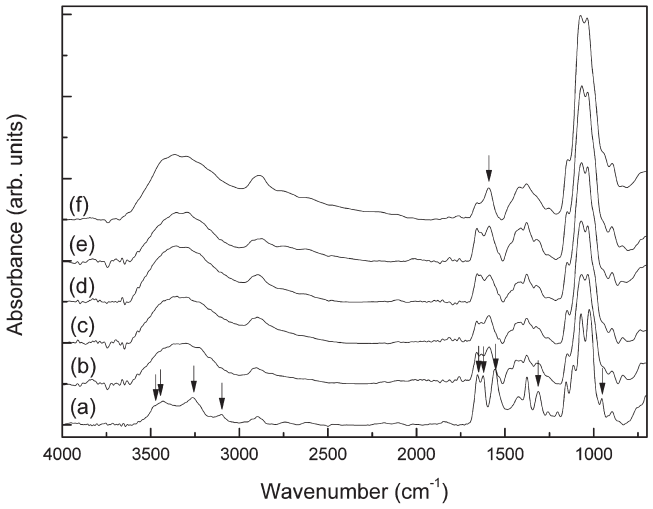

Figure 2. ATR FT-IR spectra for (a) chitin, (b) chitosan DD 73.2%, (c) chitosan DD 83.8%, (d) chitosan DD 87.3%, (e) chitosan DD 93.4%, and (f) chitosan DD 99.3%.

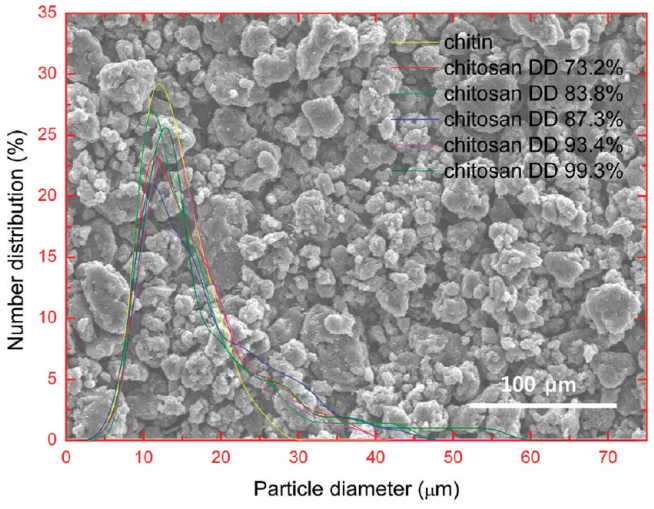

Figure 3. Size distribution of chitin and chitosans, and FE-SEM image of DD 87.3%. The average particle sizes of the ER particles are ca. 17 μm (diameter).

as the degree of *N*-deacetylation, or, simply, degree of deacetylation (DD). Generally, DD, which determines the content of free amino groups in the polysaccharides, is employed to differentiate between chitin and chitosan (Figure 1b). For instance, chitin with DD of 75% or above is generally known as chitosan.[34,35]

The FT-IR spectra of chitin exhibited the strongly parallel bands at 3432 and 3450 cm^{-1} (Figure 2a). The component absorbing at 3432 cm^{-1} may be assigned to the bond formed between the -O(3)H group and the ring oxygen in the next glucose ring. And the band at 3450 cm^{-1} most probably can be assigned to the -O(6)H stretching mode.[36] The two perpendicular bands near 3103 and 3262 cm^{-1} are most probably due to the intermolecular hydrogen bonds in CONH peptide group.[36] The peaks at 1655, 1558, and 1314 cm^{-1} can be assigned to amide I (C═O stretching), amide II (N−H in plane deformation coupled with C−N stretching), and amide III (C−N stretching coupled with NH in plane deformation) and CH_2 wagging coupled with OH in plane deformation, respectively.[37] The $C-CH_3$ wagging frequency occurred at 953 cm^{-1}.[36] After *N*-deacetylation of chitin, peaks for -NH_2 asymmetric stretching, NH stretching in interchain NH···O═C bonding, and −NH_2 scissoring appeared at 3360, 3293, and 1590 cm^{-1}, respectively.[37,38] These peaks increased with the increase of DD. Many research groups have reported on the possibility of determining DD of chitosan by comparing a peak that is proportional to the DD (measurement peak) to one that is independent of the DD (reference peak). In this study, DD of the chitosan samples was calculated using the spectra of chitosan samples, which was proposed by Domszy and Robers.[39] The computation equation is given below:

$$DD = 100 - [(A_{1655}/A_{3450}) \times 100/1.33] \quad (1)$$

where A_{1655} and A_{3450} were the absorbance at 1655 cm^{-1} of the amide I band as a measure of the *N*-acetyl group content and 3450 cm^{-1} of the hydroxyl band. The factor "1.33" denoted the value of the ratio of A_{1655}/A_{3450} for fully *N*-acetylated chitosan. It was assumed that the value of this ratio was zero for fully deacetylated chitosan and there was a rectilinear relationship between the *N*-acetyl group content and the absorbance of the amide I band. The obtained values with the IR analysis method for chitosan DD 73.2%, chitosan DD 83.8%, chitosan DD 87.3%, chitosan DD 93.4%, and chitosan DD 99.3% were 70.3, 77.6, 80.1, 85.3, and 90.2%, respectively. Methods of P.V.S.-K. titration, elemental analysis, and FT-IR are easy, fast and inexpensive to measure DD. However, there are some deviations between the measuring methods. Solid-state methods that do not require the material's dissolution present the advantage of being applicable over the entire range of DD values, both for chitin and chitosan. Solution methods are limited to soluble samples. The most widely used solid-state method for the DD determination is FT-IR spectroscopy, but some bands depend on intricate associations with the typical hydrogen-bonding networks different for each chitin polymorphic form. Despite its drawback, FT-IR spectroscopy has been often preferred because it is quick, user-friendly and low-cost method. In summary, the reason for different DD value measured by P.V.S.-K. titration, elemental analysis, and FT-IR is due to the solubility of chitosan in the solutions for the titration method, and problems of the determination of suitable bands and base lines for the FT-IR method.[40]

The particle size is important factor for comparison of the ER properties between the different chemical structures of the ER materials.[41] Figure 3 shows the particle-size distribution of the chitin and chitosans. Specific viscous behavior of ER fluids could be observed under an electric field due to the influence of particle size. And the ER effect is weak if the particles are two small, as Brownian motion tends to compete with particle fibrillation. Very large particles are also expected to display a weak ER effect, as sedimentation would prevent the particles from fibrillation bridges.[42] All ER particles have similar size distribution and the average sizes of the ER particles are ca. 17 μm (diameter).

Gelation of Chitin and Chitosan Dispersed Suspensions under Electric Fields. The formation of gels was evidenced by the data from frequency sweep experiments. A gel may be defined as a material having a loss modulus G″ considerably smaller than the storage modulus G′ for several decades of frequency, or less restrictively when G′ is greater than G″ at some fixed frequency.[43] It is intuitively expected that the cessation of tracer particle motion in a gelling system should correlate with the rheological measurements. The gelation points calculated from the bulk

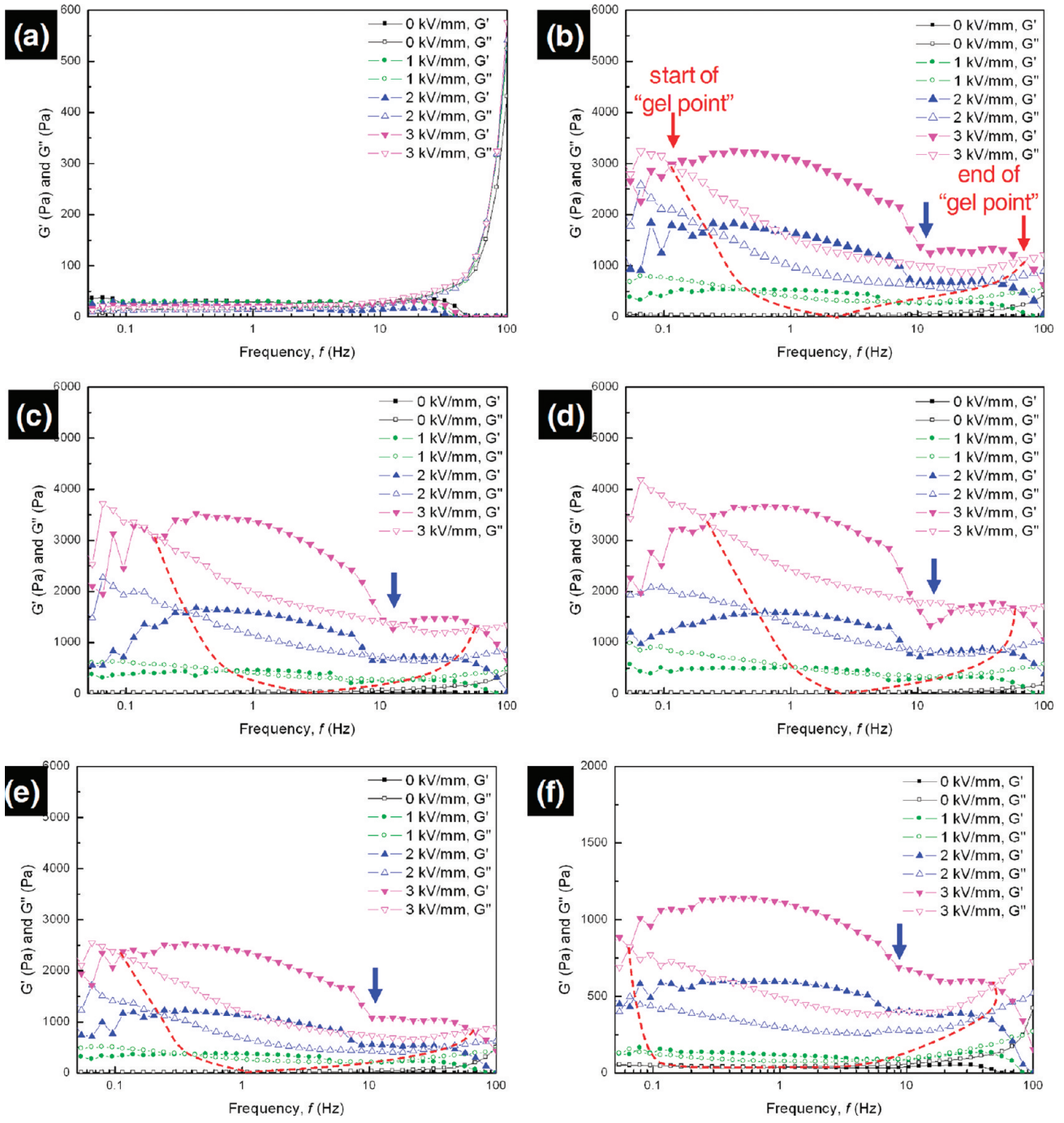

Figure 4. Effect of frequency on storage modulus (G') and loss modulus (G'') for (a) chitin, (b) chitosan DD 73.2%, (c) chitosan DD 83.8%, (d) chitosan DD 87.3%, (e) chitosan DD 93.4%, and (f) chitosan DD 99.3% at room temperature (25 °C). The particle concentration of each ER fluid is 30 vol %. Red dotted curves represent the region of the gel state at moduli curves.

rheology are indicated in Figure 4, defined as the frequency when G' is greater than G''. The chitin dispersed fluid did not show the gel state although the high electric field (3 kV/mm) was applied. However, in the case of chitosan dispersed fluids, the gel state was observed except the both low and high frequencies after the application of DC electric fields. Especially, the ER fluid of chitosan DD 83.8% showed higher modulus than any other fluids under electric fields. The region of the frequency for the gel state of all ER fluids under the electric field increased with the increase of the electric field. Red dotted curves represent the region of the gel state in the moduli curves. A noteworthy result is that the ER fluids showing low modulus under the electric field showed the gel state at the wide range of the frequency. The region of the frequency for gel state of ER fluids increased in the order of chitosan DD 99.3%, chitosan DD 93.4%, chitosan DD 73.2%, chitosan DD 83.8%, and chitosan DD 87.3% under electric fields while the modulus of the fluids increased in the reverse order. G' increased in the order of chitosan DD 99.3%, chitosan DD 93.4%, chitosan DD 73.2%, chitosan DD 83.8%, and chitosan DD 87.3%. G'' also increased in the same order. The value of G' depends on

the formation of the fibrous structure of ER particles under the electric field. The long fibrous structure is easily broken although it causes the increase of G′. G″ decreased slightly with the increase of the frequency while G′ increased at the initial step, and then decreased rapidly due to the destruction of the fibrous structure. However, in the case of chitosan DD 99.3%, its G′ increased at the initial step, and then decreased slowly because the formed fibrous structure is short and maintains its shape well for the external force. Therefore, DD 99.3% showed the gel state at the wider range of the frequency than chitosan DD 87.3%. With the increase of the electric field, the sharp decrease of G′ of ER fluids was observed (blue arrow in Figure 4) at the ca. 10 Hz of frequency. At this frequency, a region for abrupt decrease of the G′ is observed due to the destruction of the fibrous and lamellar structures of ER particles in the fluids. We suggested the model for explaining these phenomena in our previous study, and the model was well matched with the experimental data.[41]

Figure 5 shows the electrorheological property of an ER fluid visually. In the vial, 30 vol% of chitosan DD 83.8% was dispersed in silicone oil. The gap between the two stainless-steel rods was 2 mm. The two rods were connected with a high-voltage generator. After applying 3 kV/mm, there was a suspension bridge (gel state) between two rods as shown in Figure 5a. This means that the ER strength was stronger than the gravity force acting on the ER fluid. After eliminating the electric field, the bridge of the ER suspension between the two rods was broken as shown in Figure 5b.

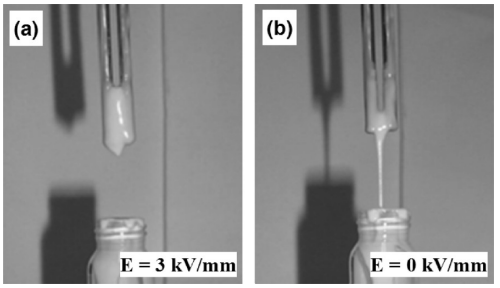

Figure 5. Observation of the ER fluid behavior between two stainless-steel rods under a 3 kV/mm DC electric field (a) after application and (b) after elimination of the DC electric filed.

The alignment of ER particles in the fluid was observed using an optical microscope with 5 vol% of chitosan DD 83.8% suspension (Figure 6a and b). The experimental cell was assembled by mounting two parallel electrodes with a 1 mm gap on a glass slide, in which a drop of well-mixed ER fluid was dispersed. The behavior of the ER fluids was observed under 3 kV/mm using a digital optical microscope. The presence of fibrils was obvious, although they were not always linear and even have double loops in some cases. These partial fibrils are though to continue to the viscosity increase, since an attempt to move one electrode relative to the order would be hindered by the drag of the dangling fibrils. ER particles are aligned under the electric field, and fibrillar shapes of the aligned ER particles flow along the fluids by shear stress.

The structural patterns of the particles suspended in the ER fluid under the electric field are depicted in Figure 6c, d. The specific increase in viscosity of an ER fluid originates from reorientation of dispersed particles whose initially random distribution transforms into a fibrillated or layered structure, giving rise to a higher viscosity. When an electric field is applied to the ER fluid, field-induced dipoles of dispersed particle attract each other and cause the particles to form chains or fibrillated structures in the direction of the field. These chains inhibit fluid flow and consequently increase apparent viscosity of the fluid in milliseconds. On the other hand, the viscosity of the fluid recovers the original state promptly by removing the applied field.[44] Generally, two different mechanisms have been proposed to explain the ER phenomena. The electrostatic polarization mechanism, proposed originally by Winslow,[45] attributes the origin of the ER effect to the field-induced polarization of the disperse phase particles relative to the continuous phase. In this model's most general form, polarization can arise from a number of charge transport mechanisms, including electronic, atomic, Debye, or

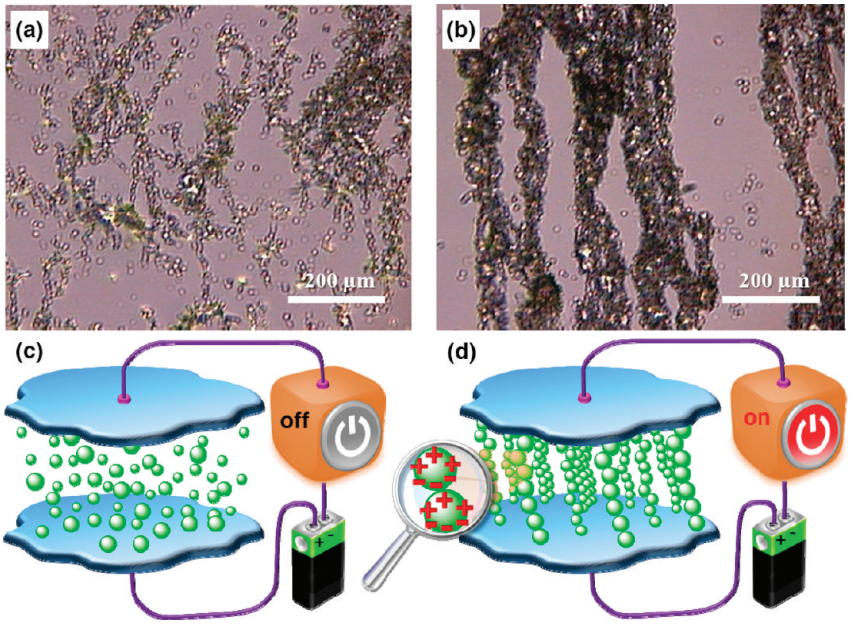

Figure 6. Optical microscopy images of (a) chitosan DD 87.3% suspension and (b) the same portion of the gel after application of a 3 kV/mm DC electric field. Structural patterns of the particles in the ER fluids; (a) before and (c) after application of a DC electric field.

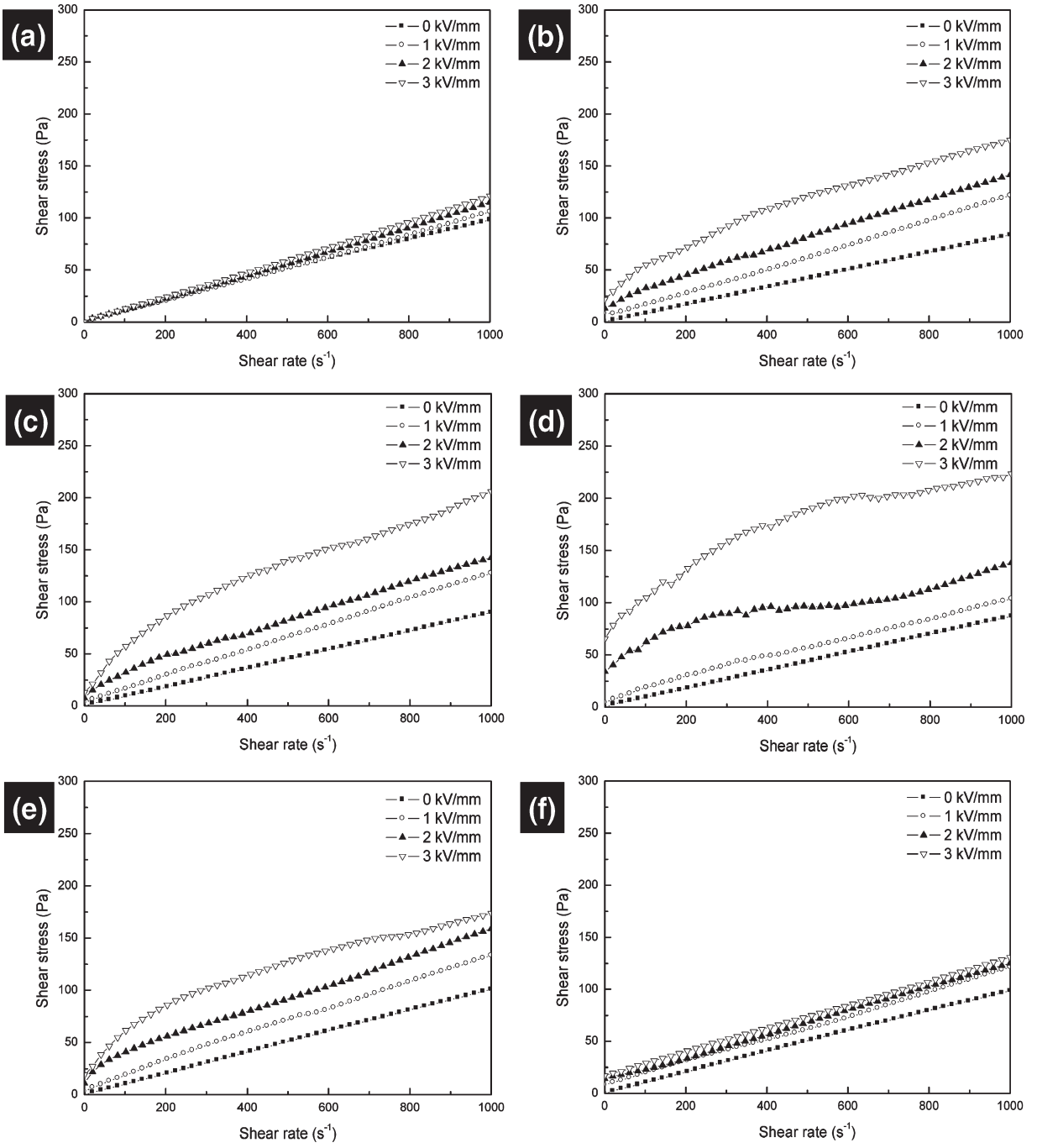

Figure 7. Shear stress versus shear rate for (a) chitin, (b) chitosan DD 73.2%, (c) chitosan DD 83.8%, (d) chitosan DD 87.3%, (e) chitosan DD 93.4%, and (f) chitosan DD 99.3% at room temperature (25 °C). The particle concentration of each ER fluid is 30 vol%.

interfacial polarization. Another proposed mechanism is the overlap of electric double layers. Each particle is surrounded by a diffuse counterion cloud that balances its charge (an electric double layer). Under the applied field, this cloud will distort and overlap with the counterion clouds of its neighbors.[46]

Electrorheological and Electrical Properties of Chitin and Chitosan Dispersed Suspensions. Shear stress is one of the critical design parameters in the ER phenomenon and has attracted considerable attention both theoretically and experimentally. Shear stress curves as a function of shear rate for chitin and chitosans dispersed suspensions under 0−3 kV/mm of the electric field are shown in Figure 7. All chitin and chitosans dispersed suspensions showed the typical Bingham plastic behavior although they showed some deviations. This means that flow is observed only after exceeding a minimum yield stress (τ_y). In the case of chitin, its fluid showed weak ER effect under an electric field. With the increase in DD, the shear stress of chitosan dispersed suspension increased under an electric field. However, after 93.4% of DD, the shear stress of chitosan dispersed suspension decreased under the electric field with the increase of DD. Chitin and highly *N*-deacetylated chitosan showed the low ER effect. These materials are a homopolymer. The chitosan

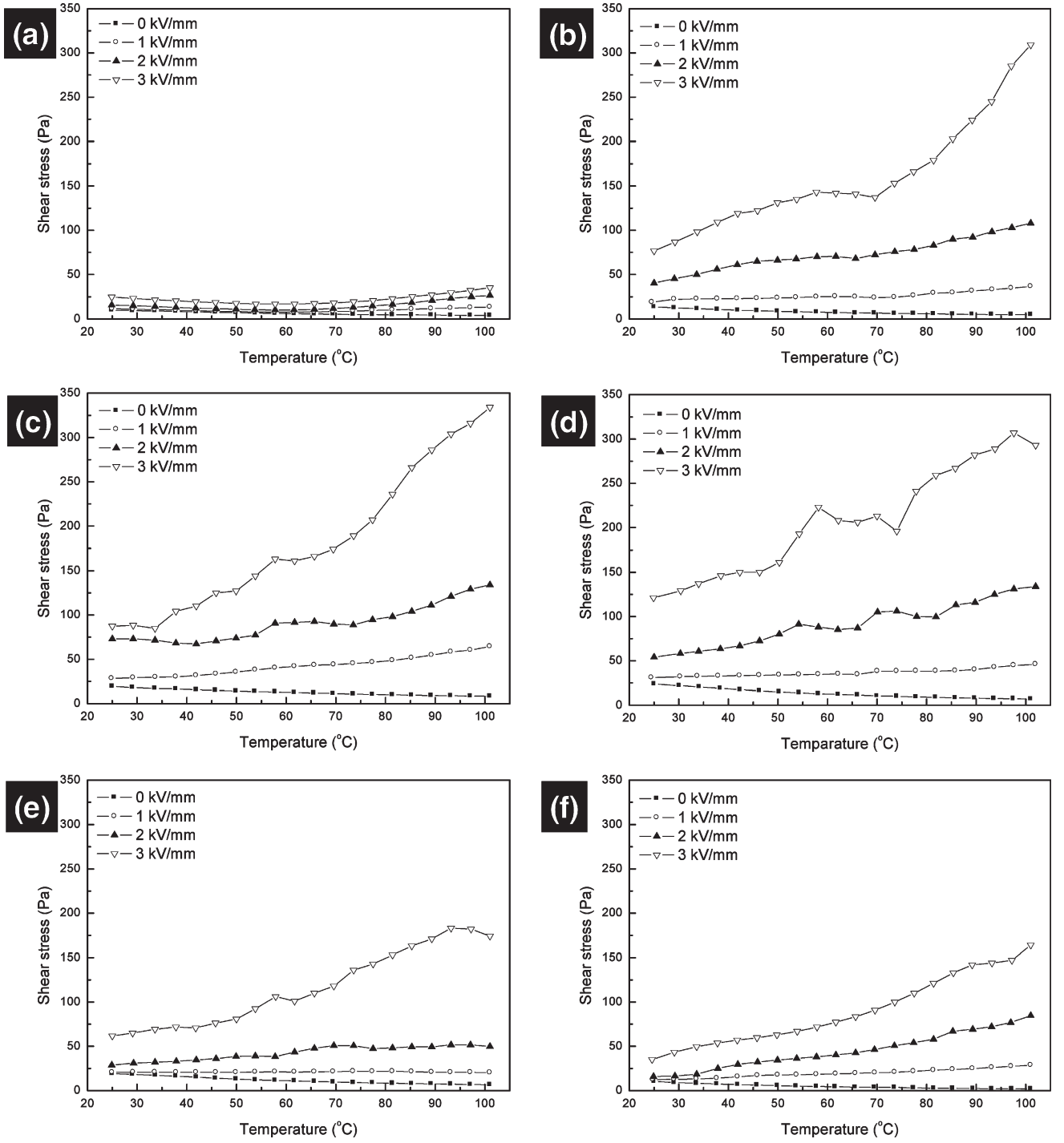

Figure 8. Effect of temperature on shear stress for (a) chitin, (b) chitosan DD 73.2%, (c) chitosan DD 83.8%, (d) chitosan DD 87.3%, (e) chitosan DD 93.4%, and (f) chitosan DD 99.3% at fixed shear rate (100 s^{-1}). The particle concentration of each ER fluid is 30 vol%.

with 87.3% of DD showing the highest ER effect is a copolymer. This result is also same with the experimental result of the effect of frequency on moduli (Figure 4). An electric field polarizes the particles, leading to the appearance of induced charge at the particle surfaces. This charge creates a dipolar field around the particle. The charges in the solvent around the particles lead to effective dipole moments for the particles. Thus, theories formulated on the basis of dielectric constant mismatches have been qualitatively successful in describing the physics of the suspensions, even in the presence of finite conductivity solvents.[44] Choi et al. measured the yield stress of the three different chitosan-oil systems (corn oil, soybean oil, and silicone oil) in the electric field, and obtained different values for different chitosan-oil systems.[47] To study the effect of chemical composition in the ER particle for the dielectric constant and the shear stress under the electric field, Unal et al. investigated polyindole/poly(vinyl acetate) conducting composites having different compositions and obtained similar results with our study.[48] There is a peak

composition in the ER particle to get high shear stress under the electric field. We think that specific chemical composition of the chitosan particle is more polarized in the silicone than other compositions. In this study, chitosan DD 87.3% showed the highest electric constant and yield stress. The charges in the silicon oil around the particles of chitosan DD 87.3% lead to more effective dipole moments for the particles than others. Herein, we can note that the copolymer is more favorable than the homopolymer to design and choose the chemical composition for ER materials.

Figure 8 shows the changes in the shear stress of chitin and chitosans suspensions under various temperatures and at constant conditions (E = 0, 1, 2, and 3 kV/mm, $\dot{\gamma}$ = 100 s^{-1}, Conc. = 30 vol%). It was observed that the shear stresses of all the suspensions examined in this work increase with the increase of temperature. The influence of temperature on shear stress may be viewed as deriving from net effect of two contributions: one is the change in the electrostatic polarization force which may either strengthen or weaken the ER effect, the other is the enhancement of Brownian thermal forces at high temperature which tends to weaken the ER effect.[49] Whether temperature increase would intensify or weaken the ER effect is really dependent on which factor would become dominant at that temperature. The results in Figure 8 suggest that the polarizability increases with temperature to an extent that dominates over the contribution from Brownian motion due to the large particle size. Moist ER suspensions are believed to have a narrow temperature range somewhat between −20 °C and +70 °C, possibly due to the water solidification and evaporation. An anhydrous ER suspension could work in a wide temperature range, however, it is limited by the large conductance at high temperature, as most anhydrous ER fluids are made from ionic materials. To remove the effect of adsorbed water on ER particles, the used chitosans were dried in a vacuum oven at 50 °C for a long time. The stable increase of shear stress was observed with the increase of temperature because there is not the water solidification or evaporation during the change of the temperature. The current density and the conductivity of all ER particles were measured, and their values were lower than 0.017 μA/cm^2 and 6 × 10^{-10} S/m at the electric field of 3 kV/mm. Therefore, the conductivity is not a significant factor for the shear stress in the case of chitin and chitosans. These materials were influenced by the polarization force dominantly, which increases with the increase in temperature.

The yield stresses obtained from various logarithmic shear stress versus shear rate curves also plotted as a function of electric field strength for ER fluids as shown in Figure 9. Electric field-induced shear stress (τ_y) is linearly related to E^2 as mentioned by Marshall et al.: $\tau_y \propto E^2$.[50] The typical correlation of the yield stress to the electric field strength at a fixed particle concentration was proposed by Klingenberg and Zukoski: $\tau_y \propto E^{\alpha}$.[51] We see that a straight line through five points with good value of R^2 is acceptable to rely on in our calculations. The α values of chitin, chitosan DD 73.2%, chitosan DD 83.8%, chitosan DD 87.3%, chitosan DD 93.4%, and chitosan DD 99.3% are 0.827, 1.306, 1.467, 1.803, 1.121, and 1.116, respectively. This result differs from the theoretical prediction that τ_y is proportional to the electric field strength E^2. The difference is due to several factors, such as particle concentration,[52] shape of the particle,[53,54] lost of ER effect,[55] and so on. Choi et al. explained the difference between theoretical value and experimental value of α using a polarization model and conductivity model.[56] In this result, the

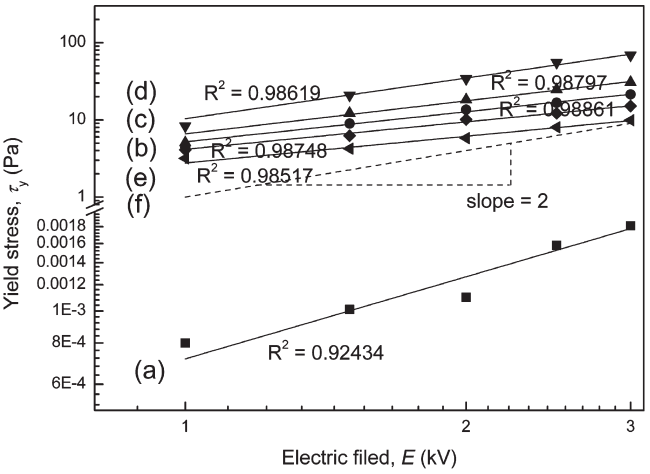

Figure 9. Log−Log plot of yield stresses versus electric field for (a) chitin, (b) chitosan DD 73.2%, (c) chitosan DD 83.8%, (d) chitosan DD 87.3%, (e) chitosan DD 93.4%, and (f) chitosan DD 99.3%.

polarization may be the main factor determining the α value. High α value of the ER fluid indicates that the fluid shows high ER effects.

The dielectric loss model is one of various models such as fibrillation model, electric double layer (EDL) model, water/surfactant bridge mechanism, polarization model, conduction model, and dielectric loss model to explain the ER phenomena.[57] Two dynamic processes were emphasized in this model. The first step is the particle polarization process, in which the particle dielectric constant in dominant. The second step is particle turning, i.e., the polarized particle could have the capability to align along the direction of the electric field. This step was determined by the particle dielectric loss. The second step is the most important one, which distinguishes the ER particle from non-ER particle. Chitin and chitosans dispersed fluids showed very low values of the conductivity. Therefore, dielectric constant is a very important factor for the chitin and the chitosans dispersed fluids as an ER fluid. Hao et al. suggested the relationship between the interfacial polarization and the particle dielectric loss.[13] The total dielectric constant, ε, can be expressed as

$$\varepsilon = \varepsilon_s + \varepsilon_I + \varepsilon_D + \varepsilon_A + \varepsilon_E = \varepsilon_s + \varepsilon_I + \varepsilon_D + \varepsilon_\infty \quad (2)$$

where ε_I, ε_D, ε_A, and ε_E are artificially regarded as the dielectric constant induced by the interfacial, the Debye, the atomic, and the electronic polarizations, respectively, ε_S is the static dielectric constant, and $\varepsilon_\infty = \varepsilon_A + \varepsilon_E$ is the high-frequency dielectric constant. Correspondingly, the total polarization of ER material, P, can be expressed as

$$P = P_I + P_D + P_A + P_E \quad (3)$$

Therefore, the high dielectric constant of fluids can exhibit high ER effects. The dielectric constant of the ER materials might be described in the following order: chitosan DD 87.3% > chitosan DD 83.8% > chitosan DD 73.2% ≫ chitosan DD 93.4% > chitosan DD 99.3% ≫ chiti,n as shown in Figure 10. This order is well-matched with the result of moduli curves against the frequency and the shear stress curves on the shear rate for ER fluids (Figures 4 and 7). In comparison to the α values in Figure 9, α is depending on the dielectric constant, ε, of the ER fluid. The high dielectric constant value of the chitosan implies that the mobile ions tend to accumulate in the chitosan. The ionic

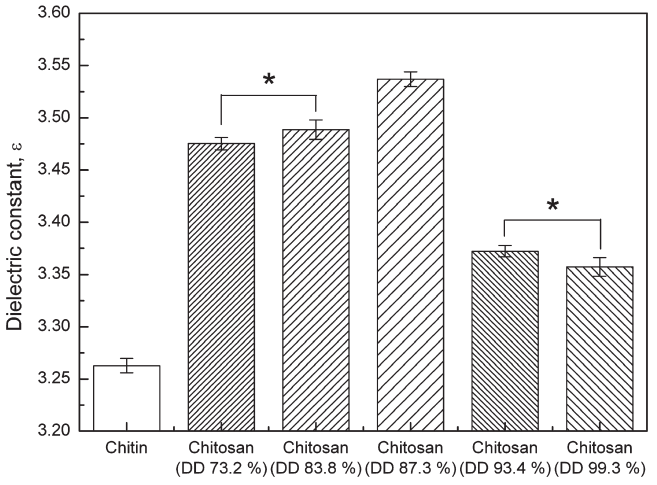

Figure 10. Dielectric constants for (a) chitin, (b) chitosan DD 73.2%, (c) chitosan DD 83.8%, (d) chitosan DD 87.3%, (e) chitosan DD 93.4%, and (f) chitosan DD 99.3% at 1 kHz of frequency. Data are presented as mean ± standard deviation, $n = 10$ (Student's t test; $^*P < 0.01$).

mobility is related with the coordination of functional groups of the chain in the chitosan.[58] The effective coordination site of functional groups of the chain depends on the conformation of the chain in the chitosan. The conformation of the chain in the chitosan is likely to be influenced by DD. The related function of the conformation of the chain in the chitosan with DD is not linear but exponential.[59] This tendency was well-matched with the value of the dielectric constant of the chitosan.

CONCLUSIONS

In this paper, we first report on the effect of the degree of deacetylation (DD) on the gelation of chitosan dispersed suspension under an electric field. We examined the particle size, the conductive, dielectric, and rheological properties of chitin and chitosan dispersed suspensions. A noteworthy result is that the region of the frequency for gel state of the ER fluids increased in the order of chitosan DD 99.3%, chitosan DD 93.4%, chitosan DD 73.2%, chitosan DD 83.8%, and chitosan DD 87.3% under electric fields while the modulus of the fluids increased in the reverse order. With the increase of DD, the shear stress of chitosan dispersed suspension increased under an electric field. However, after 93.4% of DD, the shear stress of chitosan dispersed suspension decreased under the electric field with the increase of DD. It was observed that the shear stresses of all the suspensions examined in this work increase with the increase of temperature. The stable increase in shear stress was observed with the increase of temperature because there is not the water solidification or evaporation during the change of the temperature. The current density and the conductivity of all ER particles were measured, and showed the low values under the electric field. Therefore, the conductivity may not be a significant factor for the shear stress in the case of chitin and chitosans dispersed ER fluids. These materials were influenced by the polarization force dominantly which increase with the increase of the temperature. The dielectric constant of the ER materials might be described in the following order: chitosan DD 87.3% > chitosan DD 83.8% > chitosan DD 73.2% ≫ chitosan DD 93.4% > chitosan DD 99.3% ≫ chitin. This order was well matched with the result of moduli curves against the frequency and shear stress curves on shear rate for ER fluids. In comparison to the α values which is obtained from the slope of log−log plot of the yield stresses versus electric field for ER fluids, α is depending on the dielectric constant, ε, of the ER fluid.

In brief, the results in this study indicate that ER effect of the chitosan dispersed suspension depends on the degree of deacetylation. It is expected that this work on the response of the chitosan to the electric stimulus will lay the foundation for the future application to the fabrication of the chitosan scaffold using the electrospinning process, the study on the bioelectric signal between the chitosan matrix and human cells such as stem cells, human dermal fibroblasts (hDFs), and so on in addition to electrorheological materials.

AUTHOR INFORMATION

Corresponding Author

*Phone: +82-2-958-5657. Fax: +82-2-958-5659. E-mail: uschoi@kist.re.kr.

REFERENCES

(1) Gong, J.; Zhou, Z.; Hu, X.; Wong, M.-K.; Wong, K.-W.; Du, Z. *ACS Appl. Mater. Interfaces* **2009**, *1*, 26–29.
(2) Huang, M.; Fong, C.-W.; Khor, E; Lim, L.-Y. *J. Controlled Release* **2005**, *106*, 391–406.
(3) Koev, S. T.; Dykstra, P. H.; Luo, X.; Rubloff, G. W.; Bentley, W. E.; Payne, G. F.; Ghodssi, R. *Lab Chip* **2010**, *10*, 3026–3042.
(4) Choi, S. W.; Xie, J. W.; Xia, Y. N. *Adv. Mater.* **2009**, *21*, 2997–3001.
(5) Ravi Kumar, M. N. V.; Muzzarelli, R. A. A.; Muzzarelli, C.; Sashiwa, H.; Domb, A. J. *Chem. Rev.* **2004**, *104*, 6017–6084.
(6) Choi, U. S. *Colloids Surf., A* **1999**, *157*, 193–202.
(7) Xie, T. *Nature* **2010**, *464*, 267–270.
(8) Cheng, Y.; Wu, K.; Liu, F.; Guo, J.; Liu, X.; Xu, G.; Cui, P. *ACS Appl. Mater. Interfaces* **2010**, *2*, 621–625.
(9) Bohon, K.; Krause, S. *J. Polym. Sci., Part B: Polym. Phys.* **1998**, *36*, 1091–1094.
(10) Yamaguchi, H.; Zhang, X.-R.; Niu, X.-D. *Smart Mater. Struct.* **2010**, *19*, 105032–105040.
(11) Xu, Y. L.; Qu., W. L.; Ko, J. M. *Earthquake Eng. Struct. Dyn.* **2000**, *29*, 557–575.
(12) Inoue, A.; Ide, Y.; Oda, H. *J. Appl. Polym. Sci.* **1997**, *64*, 1319–1328.
(13) Hao, T.; Kawai, A.; Ikazaki, F. *Langmuir* **1998**, *14*, 1256–1262.
(14) Tse, K.-L.; Shine, A. D. *Macromolecules* **2000**, *33*, 3134–3141.
(15) Heggset, E. B.; Dybvik, A. I.; Hoell, I. A.; Norberg, A. L.; Sørlie, M.; Fijsink, V. G. H.; Vårum, K. M. *Biomacromolecules* **2010**, *11*, 2487–2497.
(16) Laplante, S.; Turgeon, S. L.; Paquin, P. *Food Hydrocolloids* **2005**, *19*, 721–729.
(17) Ko, Y. G.; Choi, U. S.; Chun, Y. J. *Macromol. Chem. Phys.* **2008**, *209*, 890–899.
(18) Ko, Y. G.; Sung, B. H.; Choi, U. S. *Colloids Surf., A* **2007**, *305*, 120–125.
(19) Choi, U. S.; Ko, Y. G.; Kim, J. Y. *Polym. J.* **2000**, *32*, 501–504.
(20) Huo, L.; Liao, F.-H.; Li, J.-R.; Zhang, S.-H.; Zhang, O.; Ma, S.-Z.; Xu, M.-Y.; Lu, Y.-M. *Colloids Surf., A* **2008**, *316*, 125–130.
(21) Sung, J. H.; Jang, W. H.; Choi, H. J.; Jhon, M. S. *Polymer* **2005**, *46*, 12359–12365.
(22) Kean, T.; Thanou, M. *Adv. Drug Delivery Rev.* **2010**, *62*, 3–11.
(23) Tomihata, K.; Ikada, Y. *Biomaterials* **1997**, *18*, 567–575.
(24) Lamarque, G.; Viton, C.; Domard, A. *Biomacromolecules* **2004**, *5*, 1899–1907.
(25) Mao, J. S.; Cui, Y. L.; Wang, X. H.; Sun, Y.; Yin, Y. J.; Zhao, H. M.; Yao, K. D. *Biomaterials* **2004**, *25*, 3973–3981.

(26) Nam, Y. S.; Park, W. H.; Ihm, D.; Hudson, S. M. *Carbohyd. Polym.* **2010**, *80*, 291–295.
(27) Kiang, T.; Wen, J.; Lim, H. W.; Leong, K. W. *Biomaterials* **2004**, *25*, 5293–5301.
(28) Takahashi, T.; Imai, M.; Suzuki, I.; Sawai, J. *Biochem. Eng. J.* **2008**, *40*, 485–491.
(29) Iamsamai, C.; Hannongbua, S.; Ruktanonchai, U.; Soottitantawat, A.; Dubas, S. T. *Carbon* **2010**, *48*, 25030.
(30) Aranaz, I.; Harris, R.; Heras, A. *Curr. Org. Chem.* **2010**, *14*, 308–330.
(31) Desai, K.; Kit, K.; Li, J.; Zivanovic, S. *Biomacromolecules* **2008**, *9*, 1000–1006.
(32) Terayama, H. *J. Polym. Sci.* **1952**, *8*, 243–253.
(33) Kasaai, M. R.; Arul, J.; Charlet, G. *J. Polym. Sci. Pt. B-Polym. Phys.* **2000**, *38*, 2591–2598.
(34) Salmon, S.; Hudson, S. M. *J. Macromol. Sci., Rev. Macromol. Chem. Phys.* **1997**, *C37*, 199–276.
(35) Khan, T. A.; Peh, K. K.; Ch'ng, H. S. *J. Pharm. Pharmaceut. Sci.* **2002**, *5*, 205–212.
(36) Pearson, F. G.; Marchessault, R. H.; Liang, C. Y. *J. Polym. Sci.* **1960**, *43*, 101–116.
(37) Amaral, I. F.; Granja, P. L.; Barbisa, M. A. *J. Biomater. Sci.,Polym. Ed.* **2005**, *16*, 1575–1593.
(38) Valentin, R.; Bonelli, B.; Garrone, E.; Di Renzo, F.; Quignard, F. *Biomacromolecules* **2007**, *8*, 3646–3650.
(39) Domszy, J. G.; Roberts, G. A. F. *Macromol. Chem. Phys.* **1985**, *186*, 1671–1677.
(40) da Silva, R. M. P.; Mano, J. F.; Reis, R. L. *Macromol. Chem. Phys.* **2008**, *209*, 1463–1472.
(41) Ko, Y. G.; Choi, U. S.; Chun, Y. J. *J. Colloid Interface Sci.* **2009**, *335*, 183–188.
(42) Hao, T. *Adv. Mater.* **2001**, *13*, 1847–1857.
(43) Moschakis, T.; Murray, B. S.; Dickinson, E. *J. Colloid Interface Sci.* **2010**, *345*, 278–285.
(44) Halsey, T. C. *Science* **1992**, *258*, 761–766.
(45) Winslow, W. M. *J. Appl. Phys.* **1949**, *20*, 1137–1140.
(46) Parthasarathy, M.; Klingenberg, D. J. *Mater. Sci. Eng. R-Rep.* **1996**, *R17*, 57–103.
(47) Hong, C. H.; Sung, J. H.; Choi, H. J. *Colloid Polym. Sci.* **2009**, *287*, 583–589.
(48) Oz, K.; Yavuz, M.; Yilmaz, H.; Unal, H. I.; Sari, B. *J. Mater. Sci.* **2008**, *43*, 1451–1459.
(49) Hiamtup, P.; Sirivat, A.; Jamieson, A. M. *J. Colloid Interface Sci.* **2008**, *325*, 122–129.
(50) Marshall, L.; Zukoski, C. F.; Goodwin, J. W. *J. Chem. Soc.-Farady Trans. 1* **1989**, *85*, 2785–2795.
(51) Klingenberg, D. J.; Zukoski, C. F. *Langmuir* **1990**, *6*, 15–24.
(52) Sung, J. H.; Jang, W. H.; Choi, H. J.; Jhon, M. S. *Polymer* **2005**, *46*, 12359–12365.
(53) Kligenberg, D. J.; van Swol, F.; Zukoski, C. F. *J. Chem. Phys.* **1991**, *94*, 6170–6178.
(54) Kim, S. G.; Kim, J. W.; Jang, W. H.; Choi, H. J.; Jhon, M. S. *Polymer* **2001**, *42*, 5005–5012.
(55) Ko, Y. G.; Chun, Y. J.; Kim, J.-Y.; Choi, U. S. *Colloid Surf. A-Physicochem. Eng. Asp.* **2010**, *371*, 76–80.
(56) Choi, H. J.; Cho, M. S.; Kim, J. W.; Kim, C. A.; Jhon, M. S. *Appl. Phys. Lett.* **2001**, *78*, 3806–3808.
(57) Hao, T. *Adv. Colloid Interface Sci.* **2002**, *97*, 1–35.
(58) Osman, Z.; Ibrahim, Z. A.; Arof, A. K. *Carbohyd. Poym.* **2001**, *44*, 167–173.
(59) Mazeau, K.; Pérez, S.; Rinaudo, M. *J. Carbohydrate. Chem.* **2000**, *19*, 1269–1284.